Mineralogical Magazine, December 2015, Vol. 79(7), pp. 1849–1858

Bettertonite, $[Al_6(AsO_4)_3(OH)_9(H_2O)_5]\cdot 11H_2O$, a new mineral from the Penberthy Croft mine, St. Hilary, Cornwall, UK, with a structure based on polyoxometalate clusters

I.E. Grey[1,*], A.R. Kampf[2], J.R. Price[3] and C.M. Macrae[1]

[1] CSIRO Mineral Resources, Private Bag 10, Clayton South, Victoria 3169, Australia
[2] Mineral Sciences Dept., Natural History Museum of Los Angeles County, 900 Exposition Boulevard, Los Angeles, CA 90007, U.S.A.
[3] Australian Synchrotron, 800 Blackburn Road, Clayton, Victoria 3168, Australia

[*Received 27 January 2014; Accepted 19 May 2015; Associate Editor: Juraj Majzlan*]

ABSTRACT

Bettertonite, ideally $[Al_6(AsO_4)_3(OH)_9(H_2O)_5]\cdot 11H_2O$, is a new mineral from the Penberthy Croft mine, St. Hilary, Cornwall, England, UK. It occurs as tufts of white, ultrathin (sub-micrometre) rectangular laths, with lateral dimensions generally <20 μm. The laths are flattened on {010} and exhibit the forms {010}, {100} and {001}. The mineral is associated closely with arsenopyrite, chamosite, liskeardite, pharmacoalumite, pharmacosiderite and quartz. Bettertonite is translucent with a white streak and a vitreous to pearly, somewhat silky lustre. The calculated density is 2.02 g/cm^3. Optically, bettertonite is biaxial positive with $\alpha = 1.511(1)$, $\beta = 1.517(1)$, $\gamma = 1.523(1)$ (in white light). The optical orientation is $X = c$, $Y = b$, $Z = a$. Pleochroism was not observed. Electron microprobe analyses (average of 4) with H_2O calculated on structural grounds and analyses normalized to 100% gave $Al_2O_3 = 29.5$, $Fe_2O_3 = 2.0$, $As_2O_5 = 30.1$, $SO_3 = 1.8$, $Cl = 0.5$, $H_2O = 36.2$. The empirical formula, based on 9 metal atoms is $Al_{5.86}Fe_{0.26}(AsO_4)_{2.65}(SO_4)_{0.23}(OH)_{9.82}Cl_{0.13}(H_2O)_{15.5}$. Bettertonite is monoclinic, space group $P2_1/c$ with unit-cell dimensions (100 K): a = 7.773(2), b = 26.991(5), c = 15.867(3) Å, β = 94.22(3)°. The strongest lines in the powder X-ray diffraction pattern are [d_{obs} in Å(I) (*hkl*)] 13.648(100)(011); 13.505(50)(020); 7.805(50)(031); 7.461(30)(110); 5.880(20)(130); 3.589(20)(02); 2.857(14)(182). The structure of bettertonite was solved and refined to $R_1 = 0.083$ for 2164 observed ($I > 2\sigma(I)$) reflections to a resolution of 1 Å. Bettertonite has a heteropolyhedral layer structure, with the layers parallel to (010). The layers are strongly undulating and their stacking produces large channels along [100] that are filled with water molecules. The basic building block in the layers is a hexagonal ring of edge-shared octahedra with an AsO_4 tetrahedron attached to one side of the ring by corner-sharing. These polyoxometalate clusters, of composition $[AsAl_6O_{11}(OH)_9(H_2O)_5]^{8-}$, are interconnected along [100] and [001] by corner-sharing with other AsO_4 tetrahedra.

Keywords: bettertonite, new mineral, Penberthy Croft mine, polyoxometalate clusters, new aluminium arsenate.

Introduction

The Penberthy Croft mine is situated ~1.5 km from the village of Goldsithney, in the parish of St, Hilary, Cornwall, UK (50.1414°N 5.4269°W). It has historical importance as a source of copper and tin ores from the 17th century until its closure in the 1840s (Betterton, 2000; Bevins *et al*., 2010). The mine is also well known as a source of relatively rare secondary minerals, particularly Cu-Pb-Fe arsenates; in 1993 it was classified as an SSSI site (Site of Special Scientific Interest) for its mineralization. Extensive dumps around the mine have been the main source for mineral collecting.

E-mail: Ian.Grey@csiro.au
DOI: 10.1180/minmag.2015.079.7.16

To date 96 valid species have been identified (Bevins *et al.*, 2010), of which secondary hydroxyl arsenate minerals are the most prominent. Over half of the arsenates identified at Penberthy Croft are Cu-bearing species, including the only type specimen from the locality, bayldonite, $PbCu_3(AsO_4)_2(OH)_2$ (Church, 1865). Bettertonite is the second new species to be described from the Penberthy Croft mine. Considering that bettertonite has eluded discovery during over 30 years of extensive collecting at the locality, it must be considered an extremely rare secondary arsenate mineral in the oxidized zone.

The mineral and name have been approved the IMA Commission on New Minerals, Nomenclature and Classification (2014–074). The mineral is named for Mr. John Betterton (b. 1959, London) a museum geologist/mineralogist at Haslemere Educational Museum, Haslemere, Surrey, UK, for his extensive contributions to the characterization of minerals from the Penberthy Croft mine over a period of more than 30 years. Mr. Betterton has agreed to the naming of the mineral in his honour. Cotype specimens are housed in the mineralogical collections of Museum Victoria, Melbourne, Victoria, Australia, registration number M53274 and the Natural History Museum, London, registration number BM.2014,100.

In addition to its importance as a new mineral from the Penberthy Croft mine, bettertonite is of considerable crystallographic and materials science interest as a natural analogue of a polyoxometalate (POM) compound. The POMs are metal-oxygen cluster compounds with unique physical properties. The inorganic clusters can be combined in a wide variety of ways, particularly with linking organic components, to tailor the properties to particular applications in catalysis, magnetism, optics and medicine (Long *et al*., 2010). The POMs generally comprise dense aggregates of edge-shared octahedra, corner-connected to isolated tetrahedra. Commonly the clusters correspond to small elements of the *fcc* rocksalt structure. Frequently encountered examples include the Lindqist molybdate anion, $[Mo_6O_{19}]^{2-}$, the Anderson ion, $[M'M_6O_{24}]^{n-}$, the decavanadate ion, $[V_{10}O_{28}]^{6-}$ and the Keggin ion, $[XM_{12}O_{40}]^{n-}$, where X is a tetrahedral cation. Because of their technological importance, research on POMs has increased almost exponentially over recent decades and hundreds of new materials are synthesized each year (Lopez *et al*., 2012). Surprisingly, there are very few known mineral examples of POMs (Kampf *et al*., 2014*a*). The pascoite family of minerals contain the decavanadate ion (Kampf *et al*., 2014*b*) and ophirite contains tri-lacunary Keggin anions (Kampf *et al*., 2014*c*). The structure of bettertonite can be described simply in terms of POMs, as will be described below.

Occurrence

The Penberthy Croft mine is situated in Devonian metasediments consisting of lower-grade-greenschist facies slates between the Land's End and Godolphin granite masses. A series of interbedded metabasic rocks strikes east-west within the mine. The main Penberthy lode strikes east-west and dips to the south. The lode is associated with a rhyolite porphyry elvan dyke and cross-course structures, and is probably related to a shear zone.

The mineralization is of a multi-stage, polymetallic and hydrothermal character. The deposit consists of several, but distinct overlapping assemblages: Minor, burial-related quartz-albite-anatase-monazite veins of a pre-tectonic, metamorphic origin; main-stage high-temperature Sn-Cu-As-W veins; later lower-temperature Pb-Zn sulfide mineralization; and a late-stage, low-temperature Fe-Mn mineralization. Subsequent supergene oxidation and weathering of lodes resulted in formation of complex gossans with oxide and supergene enrichment zones. Post-mining formation of other minerals both underground and on the dumps has resulted in an extraordinarily large variety of mineral species within a small area. The mineralization formed over a very wide period of time extending from the Upper Palaeozoic through to the Cenozoic. The most detailed and comprehensive work covering the economic history, geology and mineralization of this deposit is provided by Betterton (2000).

Specimens containing bettertonite were collected by John Betterton during the early 2000s in two separate parts (~700 m apart) of the mine dumps. They consist mainly of fresh, white massive vein quartz and massive, granular to platy dark green chamosite with fresh massive grey arsenopyrite, as shown in Fig. 1. Minor massive blebs of chalcopyrite and cassiterite are also present. Bettertonite generally occurs as bright white, lustrous, thin blades, sprays and laths. They form radiating crystal groups that line and infill interconnecting and isolated cavities in quartz and chamosite; less commonly the mineral is found on fresh to slightly tarnished (Fe-stained) subhedral arsenopyrite crystals. Cavities range in size from

FIG. 1. Optical image of bettertonite (white) on quartz (white, translucent), with associated chamosite (green) and arsenopyrite (steel grey). Field of view is 6 mm. Specimen Number PC238. John Betterton Collection. Image Robert Neller.

<1 mm to up to 4 mm. Bettertonite has also been found completely covering small quartz crystals in some cavities. The mineral is associated closely with arsenopyrite, chamosite, liskeardite, pharmacoalumite, pharmacosiderite and quartz. Brochantite, cassiterite and chalcopyrite also occur on specimens but are not in direct contact with the mineral.

The arsenate mineral assemblage at Penberthy Croft is interpreted as having formed from prolonged oxidation of primary sulfides in the upper parts of lodes and veins within the mine and on dump material (Betterton, 2000). Much of the supergene alteration is post mining. It is possible that bettertonite, like liskeardite (Grey *et al*., 2013), has formed from leaching and the replacement of Al for Fe in pharmacosiderite.

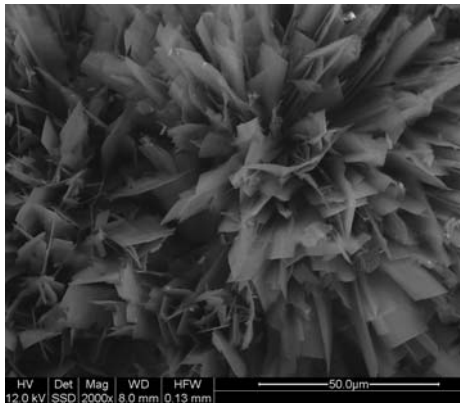

FIG. 2. Backscattered electron image of bettertonite laths.

Appearance, physical and optical properties

Bettertonite crystals occur as tufts of white, ultrathin (sub-micrometre) rectangular laths, with lateral dimensions generally <20 μm, (Fig. 2). The laths are flattened on {010} and exhibit the forms {010}, {100} and {001}. The crystals are typically present as very thin flattened blades, sprays and laths, forming closely packed radiating rough spheres, clusters and hemispheres. Curvature of the laths is common. The very small size and especially the thinness of the crystals made it difficult to measure some of the physical properties.

Bettertonite is translucent with a white streak and a vitreous to pearly, somewhat silky lustre. It shows perfect basal cleavage parallel to (010). The crystals are flexible, with irregular fracture. The calculated density is 2.02 g/cm^3 using the empirical formula. Optically, bettertonite is biaxial positive with $\alpha = 1.511(1)$, $\beta = 1.517(1)$, $\gamma = 1.523(1)$ (in white light). The 2V could not be measured but 2V(calc.) is 60.2°. The optical orientation is $X = c$, $Y = b$, $Z = a$. Pleochroism was not observed. The Gladstone-Dale compatibility index is –0.047, classed as good (Mandarino, 1981).

Chemical analysis

Crystals of bettertonite were analysed using wavelength dispersive spectrometry on a JEOL JXA 8500F Hyperprobe operated at an accelerating voltage of 12 kV and a beam current of 1 nA. The beam was defocused to 2 μm. As is typical of highly hydrated phases with weakly held H_2O, bettertonite partially dehydrates under vacuum in the electron microprobe. This H_2O loss results in higher concentrations of the remaining constituents than are to be expected for the fully hydrated phase. Because insufficient material is available for a direct determination of H_2O, it has been calculated based on the structure determination. The analysed constituents have then been normalized to provide a total of 100% when combined with the calculated H_2O. Analytical results from analysis of four crystals (four analyses) are given in Table 1.

The empirical formula, based on 9 cations (Al^{3+} + Fe^{3+} + As^{5+} + S^{6+}) per asymmetric unit, and with OH adjusted for charge balance is: $Al_{5.86}Fe_{0.26}(AsO_4)_{2.65}(SO_4)_{0.23}(OH)_{9.82}Cl_{0.13}(H_2O)_{15.5}$. The simplified structural formula is $[Al_6(AsO_4)_3(OH)_9(H_2O)_5] \cdot 11H_2O$, which requires Al_2O_3 30.1, As_2O_5 33.7, H_2O 36.2, total 100.0 wt.%.

TABLE 1. Electron microprobe analytical data for bettertonite.

Constituent	Wt.%	Range	SD	Norm. wt.%	Probe standard
Al_2O_3	35.8	34.5–36.1	0.9	29.5	$AlPO_4$
Fe_2O_3	2.45	1.93–2.82	0.32	2.0	scorodite
As_2O_5	36.5	35.6–37.7	0.8	30.1	scorodite
SO_3	2.19	1.18–2.60	0.58	1.8	pyrite
Cl	0.56	0.29–0.89	0.21	0.5	NaCl
Ox equiv	–0.13			–0.1	
H_2O*				36.2	
Total				100.0	

*Based on a refined crystal structure, with 6 Al, 3 As and 37 anions in the asymmetric unit.

TABLE 2. Powder X-ray diffraction data for bettertonite.

I_{rel}	d_{meas}	d_{calc}	h	k	l
100	**13.648**	**13.687**	**0**	**1**	**1**
50	**13.505**	**13.479**	**0**	**2**	**0**
50	**7.805**	**7.821**	**0**	**3**	**1**
30	**7.461**	**7.466**	**1**	**1**	**0**
10	6.848	6.843	0	2	2
3	6.750	6.732	1	2	0
5	6.599	6.592	1	1	1
20	**5.880**	**5.877**	**1**	**3**	**0**
12	5.622	5.628	$\bar{1}$	1	2
4	5.375	5.374	1	0	2
4	5.274	5.270	1	1	2
4	5.131	5.139	0	4	2
7	4.918	4.913	$\bar{1}$	4	1
12	4.291	4.288	$\bar{1}$	2	3
7	4.203	4.201	1	4	2
7	3.886	3.889	1	6	0
8	3.740	3.743	0	7	1
20	**3.589**	**3.588**	$\bar{2}$	**0**	**2**
7	3.466	3.465	0	7	2
10	3.438	3.434	2	3	1
3	3.252	3.254	$\underline{2}$	4	1
6	3.199	3.201	$\bar{1}$	7	2
7	3.086	3.085	1	6	3
4	2.938	2.939	2	6	0
14	2.857	2.855	1	8	2
3	2.742	2.741	$\underline{1}$	9	1
4	2.571	2.573	$\bar{3}$	1	1
5	2.544	2.543	3	2	0
4	2.418	2.418	3	4	0
3	2.374	2.376	$\underline{3}$	2	2
2	2.331	2.331	$\bar{3}$	5	1
3	2.305	2.306	$\underline{2}$	6	4
5	2.240	2.240	$\bar{3}$	6	1
5	2.238	2.238	0	2	7

The strongest lines are given in bold.

Crystallography

Powder X-ray diffraction

Powder X-ray diffraction (PXRD) data were collected using a Philips diffractometer with graphite-monochromated Co$K\alpha$ radiation. The X-ray tube was operated at 40 kV and 40 mA with 1° divergent and scatter slits, a 0.3-mm receiving slit and soller slits. Step scan intensity data were collected in the 2θ range 5 to 60°, using a step size of 0.02° and a step counting time of 15 s. Indexing of the PXRD data using the *Ito* method as implemented by Visser (1969) gave a monoclinic cell, which was subsequently confirmed from synchrotron studies on a single crystal. Refinement of 34 2θ values using *CELLREF* (Laugier and Bochu, 2000) gave the following cell parameters: a = 7.788 (3), b = 26.957(7), c = 15.925 (8) Å, β = 93.9(1)° and V = 3336(4) Å^3. The systematic absences are consistent with space group $P2_1/c$. The powder data are presented in Table 2.

Single-crystal studies

A rectangular lath, measuring ~0.02 mm × 0.01 mm × 0.001 mm was used for a data collection at 100 K on the microfocus beamline MX2 at the Australian Synchrotron, λ = 0.7107 Å. The extreme thinness and curvature of the crystal resulted in very weak diffraction data and a high mosaicity. A relatively large R_{int} of 0.15 was obtained for merging equivalent reflections at a data resolution of 1.0 Å ($2\theta_{max}$ = 40°).

The structure was solved using *SHELXT* and refined using *SHELXL* (Sheldrick, 2008) within the *WinGX* program suite (Farrugia, 2012). Partially occupied water molecule sites were located in

TABLE 3. Crystal data and structure refinement for bettertonite.

Formula	$[Al_6(AsO_4)_3(OH)_9(H_2O)_5]\cdot 11H_2O$
Temperature	100 K
Wavelength	0.71073 Å
Crystal system	Monoclinic
Space group	$P2_1/c$
Unit-cell dimensions	a = 7.773(2) Å
	b = 26.991(5) Å
	c = 15.867(3) Å
	β = 94.22(3)°
Volume	3319.9(12) Å^3
Z	4
Density (calculated)	2.02 g/cm^3
Absorption coefficient	3.264 mm^{-1}
Crystal size	0.02 mm × 0.01 mm × 0.001 mm
Theta range	1.49 to 19.98°
Index ranges	–7<=h<=7, –25<=k<=25, –14<=l<=14
Reflections collected	22,571
Independent reflections	3005 [*R(int)* = 0.156]
Completeness to θ = 19.98°	97.1%
Refinement method	Full-matrix least-squares on F^2
Data / restraints / parameters	3005 / 0 / 414
Reflections with $I > 2\sigma(I)$	2164
Goodness-of-fit on F^2	0.954
Final R indices [$I > 2\sigma(I)$]	R_1 = 0.083, wR_2 = 0.212
R indices (all data)	R_1 = 0.118, wR_2 = 0.241
Extinction coefficient	0.0017(4)
Largest diff. peak and hole	1.16 and –0.68 e.Å^{-3}

difference-Fourier maps. The final refinement, incorporating anisotropic displacement parameters for all heteropolyhedral layer atoms and an overall isotropic displacement parameter for the partially occupied interlayer water sites, converged to R_1 = 0.083 for 2164 observed reflections ($I > 2\sigma(I)$) to a resolution of 1.0 Å. Further details of the data collection and structure refinement are given in Table 3. The refined coordinates, equivalent isotropic displacement parameters and site occupancies are given in Table 4. Included in Table 4 are bond-valence sums obtained using the program *BVCALC* in *WinGX* (Farrugia, 2012). Tables of anisotropic displacement parameters and observed and calculated structure factors have been deposited with the Principal Editor of *Mineralogical Magazine* and are available from www.minersoc.org/pages/e_journals/dep_mat_mm.html.

Description of the structure

Bettertonite has a heteropolyhedral layer structure, with the layers parallel to (010) as shown in Fig. 3. The layers comprise hexagonal rings of edge-shared Al-centred octahedra that are interconnected by corner-sharing with AsO_4 tetrahedra. The layers are strongly undulating and their stacking produces large channels along [100], centred on the cell axes at y = 0, z = ½ and y = ½, z = 0. The channels are filled with water molecules, which become disordered progressively as their distance from the channel walls increases. Polyhedral bond lengths, reported in Table 5, are within normal ranges for Al-centred octahedra and As-centred tetrahedra.

The H atoms could not be located in the structure refinement, but bond valence (BV) calculations allow an assignment of coordinated water molecules and hydroxyl ions. The BV values in Table 4 are consistent with eight hydroxyl anions, OH1–OH8, each of which is shared between two Al atoms, and six coordinated water molecules, OW1–OW6, each of which is coordinated to only one Al atom. Low BV sums are calculated for O2 and O5, the unshared apical anions of tetrahedra centred on As1 and As2 respectively, shown in Fig. 4. These two anions are acceptor atoms in multiple H bonds (OW1, OH1, OH7···O2 = 2.56, 2.70, 2.71 Å; OW4, OW3,

TABLE 4. Refined coordinates, equivalent isotropic displacement parameters, site occupancy factors (SOF) and bond-valence sums (BV) for bettertonite.

Atom	SOF	*x*	*y*	*z*	U_{equ} (Å^2)	BV
Heteropolyhedral layer sites						
As1	1	0.0063(2)	0.60174(9)	0.55315(14)	0.0292(7)	5.31
As2	1	0.5135(2)	0.68822(9)	0.52147(14)	0.0311(8)	5.18
As3	1	0.2977(3)	0.72405(9)	0.25882(14)	0.0311(8)	5.22
Al1	1	0.6365(7)	0.5759(2)	0.4678(4)	0.0272(16)	2.82
Al2	1	0.3727(7)	0.6227(2)	0.3561(4)	0.0265(16)	2.78
Al3	1	0.1442(7)	0.7146(2)	0.6055(4)	0.0257(16)	2.75
Al4	1	0.1176(7)	0.6923(2)	0.4238(4)	0.0276(16)	2.76
Al5	1	0.6653(7)	0.6005(3)	0.6519(4)	0.0299(17)	2.82
Al6	1	0.4245(7)	0.6684(3)	0.7199(4)	0.0314(17)	2.76
O01	1	0.9053(15)	0.6050(5)	0.6405(8)	0.024(3)	1.82
O02	1	1.1815(15)	0.5672(6)	0.5672(10)	0.040(4)	1.36
O03	1	0.8785(15)	0.5796(5)	0.4731(8)	0.028(3)	1.82
O04	1	1.0679(15)	0.6597(5)	0.5293(8)	0.026(3)	2.02
O05	1	0.653(2)	0.7300(9)	0.5015(14)	0.086(7)	1.54
O06	1	0.3910(15)	0.6980(5)	0.6024(9)	0.032(4)	2.00
O07	1	0.3662(15)	0.6772(5)	0.4386(8)	0.026(3)	1.96
O08	1	0.6195(18)	0.6338(5)	0.5428(8)	0.035(4)	2.05
O09	1	0.1574(15)	0.7335(5)	0.3310(8)	0.032(4)	1.85
O10	1	0.1957(16)	0.7256(5)	0.1626(9)	0.033(4)	1.80
O11	1	0.3882(18)	0.6681(5)	0.2681(8)	0.032(4)	1.82
O12	1	0.4545(15)	0.7671(6)	0.2667(9)	0.037(4)	1.73
OH1	1	0.3985(15)	0.5746(5)	0.4434(8)	0.024(3)	0.99
OH2	1	0.6111(16)	0.6145(5)	0.3692(9)	0.034(4)	1.01
OH3	1	0.6365(15)	0.5456(5)	0.5765(8)	0.026(3)	0.92
OH4	1	0.1332(15)	0.6327(5)	0.3647(8)	0.029(3)	0.99
OH5	1	0.1836(15)	0.6758(5)	0.7020(8)	0.030(4)	1.01
OH6	1	0.1403(15)	0.7449(5)	0.4996(9)	0.031(4)	1.03
OH7	1	0.4344(15)	0.6035(5)	0.6769(8)	0.028(3)	1.00
OH8	1	0.6616(15)	0.6597(5)	0.7117(8)	0.033(4)	1.02
OW1	1	0.6486(16)	0.5141(5)	0.4107(9)	0.033(4)	0.46
OW2	1	0.3223(16)	0.5697(6)	0.2750(9)	0.038(4)	0.41
OW3	1	0.9063(15)	0.7252(5)	0.6225(8)	0.030(4)	0.46
OW4	1	0.8751(16)	0.6993(6)	0.3949(8)	0.035(4)	0.45
OW5	1	0.7185(17)	0.5586(6)	0.7480(8)	0.037(4)	0.45
OW6	1	0.4115(17)	0.6424(6)	0.8301(9)	0.040(4)	0.47
Interlayer water molecules						
W1	1	0.0791(17)	0.5180(5)	0.3646(9)	0.033(4)	
W2	1	0.7547(17)	0.7811(5)	0.7367(9)	0.038(4)	
W3	1	0.944(2)	0.8175(7)	0.3330(11)	0.060(5)	
W4	1	0.417(3)	0.6886(8)	0.9772(13)	0.079(6)	
W5	0.62(4)	0.546(5)	0.6439(13)	1.123(2)	0.080(6)	
W6	0.5(1)	0.859(6)	0.619(4)	0.228(4)	0.080(6)	
W7	0.54(4)	0.484(5)	0.5447(14)	0.864(2)	0.080(6)	
W8	0.44(5)	0.840(7)	0.467(2)	0.259(3)	0.080(6)	
W9	0.54(4)	0.010(5)	0.6468(15)	0.103(2)	0.080(6)	
W10	0.50(4)	1.007(5)	0.5830(15)	0.854(3)	0.080(6)	
W11	0.27(4)	0.658(11)	0.505(3)	0.170(6)	0.080(6)	
W12	0.23(4)	0.471(11)	0.495(3)	0.790(6)	0.080(6)	

(continued)

TABLE 4. (*contd*.)

Atom	SOF	*x*	*y*	*z*	U_{equ} (Å^2)	BV
W13	0.34(4)	0.433(9)	0.626(2)	0.101(4)	0.080(6)	
W14	0.33(4)	0.784(8)	0.799(3)	0.486(4)	0.080(6)	
W15	0.25(4)	0.836(11)	0.836(4)	0.494(6)	0.080(6)	
W16	0.22(4)	0.191(12)	0.566(4)	0.114(6)	0.080(6)	
W17	0.40(4)	0.120(8)	0.626(2)	0.121(3)	0.080(6)	
W18	0.26(4)	0.928(12)	0.452(3)	0.231(6)	0.080(6)	
W19	0.22(4)	0.576(13)	0.504(4)	0.114(7)	0.080(6)	
W20	0.22(4)	0.782(14)	0.504(5)	0.239(6)	0.080(6)	
W21	0.24(4)	0.687(12)	0.532(4)	0.240(6)	0.080(6)	
W22	0.5(1)	0.867(7)	0.598(4)	0.248(5)	0.080(6)	
W23	0.17(4)	0.555(15)	0.531(4)	0.955(7)	0.080(6)	
W24	0.17(4)	0.659(15)	0.550(5)	0.093(7)	0.080(6)	

W4···O5 = 2.64, 2.65, 2.87 Å), which increase their BV sums to close to 2. The composition of the heteropolyhedral layers, based on the BV assignments, is $[Al_6(AsO_4)_3(OH)_8(H_2O)_6]^{1+}$, whereas charge balance requires $Al_6(AsO_4)_3(OH)_9(H_2O)_5$. The difference could be due to incomplete occupancy of cation sites, although there was no clear evidence of this from site occupancy refinements. A more likely explanation is that the extra hydroxyl ion per formula unit is distributed statistically over the coordinated water sites.

A projection of the heteropolyhedral layer along [010] in Fig. 4 shows that the basic building block is a hexagonal ring of edge-shared octahedra with an As2O$_4$ tetrahedron attached to one side of the ring by corner-sharing. These anionic clusters, of composition $[AsAl_6O_{11}(OH)_9(H_2O)_5]^{8-}$, ≡ $[AsAl_6\Phi_{25}]$, Φ = O, OH, H_2O, are interconnected along [100] and [001] by corner-sharing with other AsO_4 tetrahedra. This type of cluster has recently been reported as a new polyoxometalate building block for the cluster composition $[VMo_6O_{25}]^{9-}$ (Gao *et al*., 2014). The cluster also occurs in the ε isomer of the Keggin cluster, $[\varepsilon\text{-}XM_{12}O_{40}]^{n-}$ (Lopez *et al*., 2012). In this case four hexagonal rings are fused by edge-sharing into a tetrahedral cluster with an XO_4 tetrahedron in the centre of the cluster, corner-sharing to all four rings. The composition of the heteropolyhedral layer in bettertonite can be represented in terms of the

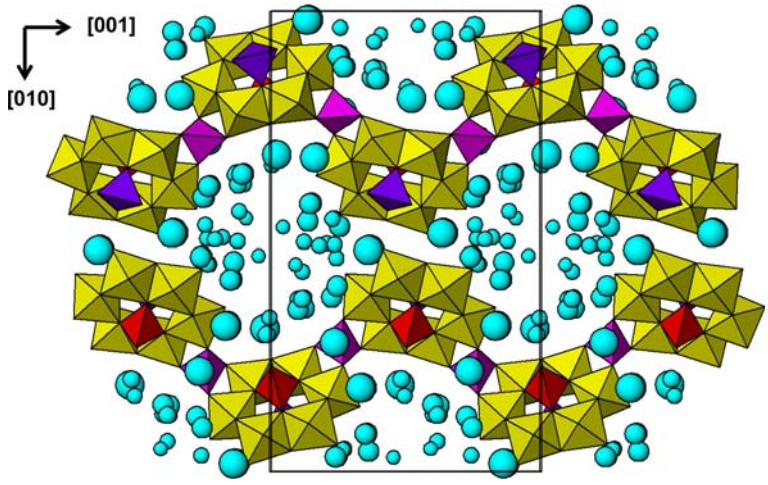

FIG. 3. Projection of the bettertonite structure along [100]. Interlayer water molecules are shown as blue spheres, with sizes proportional to the site occupancies.

TABLE 5. Polyhedral bond distances (Å) for bettertonite.

As1–O1	1.65(1)	As2–O5	1.61(2)	As3–O9	1.66(1)
–O2	1.65(1)	–O6	1.67(1)	–O10	1.67(1)
–O3	1.66(1)	–O7	1.70(1)	–O11	1.67(1)
–O4	1.68(1)	–O8	1.70(1)	–O12	1.68(1)
Al1–OH1	1.86(1)	Al2–OH2	1.86(1)	Al3–OH5	1.86(1)
–O3	1.88(1)	–O11	1.87(1)	–OH6	1.87(1)
–OH2	1.88(1)	–OH1	1.90(1)	–O10	1.88(1)
–OH3	1.91(1)	–OH4	1.90(1)	–OW3	1.91(1)
–OW1	1.90(1)	–OW2	1.94(1)	–OH8	1.98(1)
–O8	1.98(1)	–O7	1.97(1)	–O6	1.97(1)
Al4–OH6	1.86(1)	Al5–OH7	1.87(1)	Al6–OH8	1.87(1)
–OH4	1.87(1)	–OH8	1.86(1)	–OH7	1.88(2)
–O9	1.89(1)	–O1	1.89(1)	–O12	1.90(2)
–OW4	1.92(1)	–OH3	1.91(1)	–OH5	1.88(1)
–O4	1.95(1)	–OW5	1.92(1)	–OW6	1.89(2)
–O7	1.97(1)	–O8	1.96(1)	–O6	2.03(2)

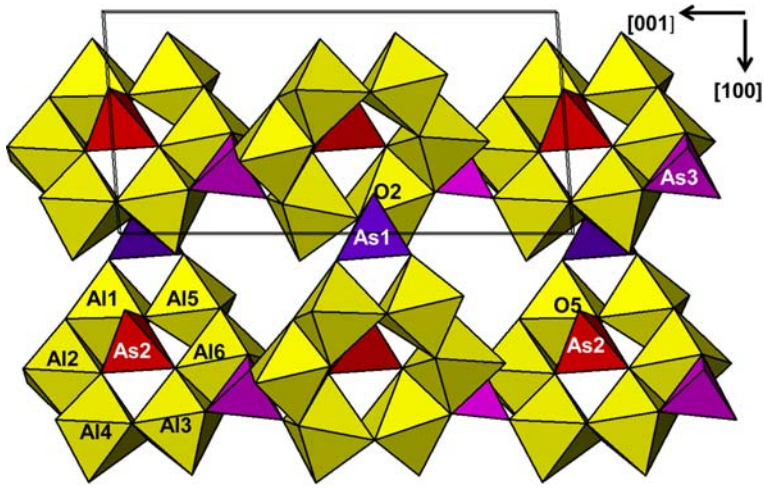

FIG. 4. The (010) heteropolyhedral layer in bettertonite, viewed normal to the layer. Metal atom sites are labelled, as well as unshared apical anions of the $As1O_4$ and $As2O_4$ tetrahedra.

clusters by: $[AsAl_6O_{11}(OH)_9(H_2O)_5]^{8-}[As]^{5+}$ $[AsO]^{3+}$. The $[AsO]^{3+}$ refers to the As1-centred tetrahedron, which has an unshared apical oxygen, O2, while the $[As]^{5+}$ refers to the As3-centred tetrahedron, for which all four vertices are corner-shared with $Al\Phi_6$ octahedra, as shown in Fig. 4. The bettertonite layers are shown in projection along [001] in Fig. 5. This view illustrates that the hexagonal rings are inclined at ~40° to the *a* axis, and that successive [100] columns of clusters along [001] are inclined in opposite directions.

At the Penberthy Croft mine, bettertonite is found in close association with liskeardite, another secondary aluminium arsenate with a similar composition, $[Al_{32}(AsO_4)_{18}(OH)_{42}(H_2O)_{22}]\cdot 52H_2O$ (Grey *et al*., 2013). Liskeardite has a lower [Al]/[As] atomic ratio of 1.78 compared with 2 for bettertonite but a similar high water content of >30 wt.%. Although the structures of the two minerals have a 7.8 Å axis in common they differ considerably. In contrast to the layer structure of bettertonite, likeardite has an open framework structure in which intersecting

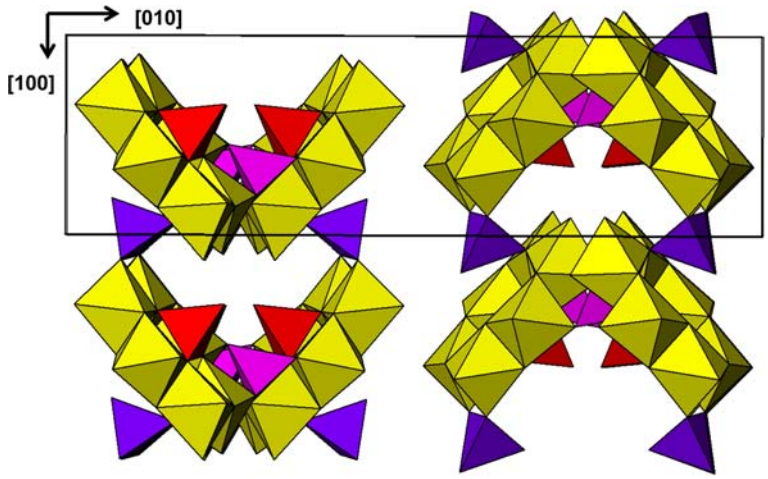

FIG. 5. The heteropolyhedral layers in bettertonite, viewed along [001].

heteropolyhedral slabs form 17.4 Å × 17.4 Å channels parallel to the 7.8 Å axis. The framework comprises columns of pharmacoalumite type, intergrown with chiral chains of six *cis* edge-shared octahedra that are decorated by corner-connected AsO_4 tetrahedra (Grey *et al*., 2013). There is a close structural relationship between the spiral chains in liskeardite and the [100] columns of hexagonal rings in liskeardite, see Fig. 6. The two types of structural elements can be interconverted by the relocation of just one Al atom per cluster as shown by the arrows in Fig. 6. The topology of the corner-linking between AsO_4 tetrahedra and the $Al\Phi_6$ octahedra is identical in both structures, as is the degree of inclination of the octahedral clusters relative to the 7.8 Å axis.

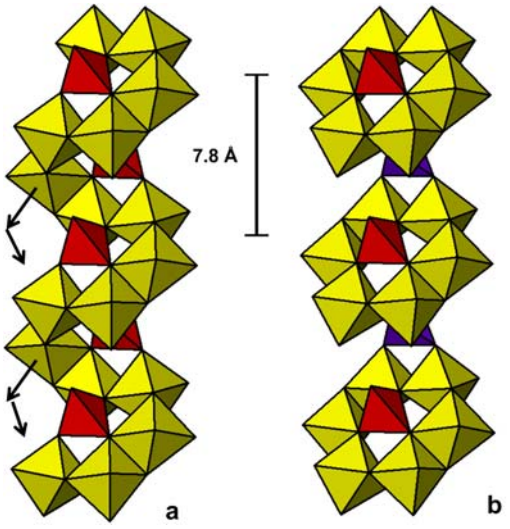

FIG. 6. A comparison of (*a*) chiral chains of edge-shared octahedral in liskeardite with (*b*) [100] columns of $[AsAl_6\Phi_{25}]$ in bettertonite. Arrows show the movement of an Al atom per cluster required to transform (*a*) to (*b*).

Our ongoing structural studies will focus on related secondary aluminium arsenate minerals which are microcrystalline and not readily amenable to single crystal analysis. These include a possible polytype of bettertonite from the Penberthy Croft mine, and the basic arsenate mineral bulachite, $Al_2(AsO_4)(OH)_3 \cdot 3H_2O$. The structure of the latter mineral has remained unsolved since its discovery over 30 years ago (Walenta, 1983). Both minerals have a 7.8 Å axis in common with liskeardite and bettertonite, so their structure determination may be assisted by the new structural data for the latter two minerals.

Acknowledgements

Many thanks to John Betterton for supplying specimens from the Penberthy Croft mine for study. Cameron Davidson and Matthew Glenn are thanked for sample preparation and scanning electron microscopy assistance. Robert Neller is thanked for the optical image in Fig. 1. The single-crystal data were collected at the macromolecular MX2 beamline at the Australian Synchrotron, Clayton, Victoria.

References

Betterton, J. (2000) Famous mineral localities: Penberthy Croft mine, St. Hilary, Cornwall, England, UK. *Journal of Mines and Minerals*, **20**, 7–37.

Bevins, R.E., Young, B., Mason., J.S., Manning, D.A.C. and Symes, R.F. (2010) *Mineralization of England and Wales, Geological Conservation Review Series, No 36.* Joint Nature Conservation Committee, Peterborough [pp. 496–499].

Church, A.H. (1865) Chemical researches on some new and rare Cornish minerals. *Journal of the Chemical Society*, **18**, 259–268.

Farrugia, L.J. (2012) WinGX and ORTEP for Windows: an update. *Journal of Applied Crystallography*, **45**, 849–854.

Gao, Q., Li, F., Wang, Y., Xu, L., Bai, J. and Wang, Y. (2014) Organic functionalization of polyoxometalate in aqueous solution: self-assembly of a new building block of $\{VMo_6O_{25}\}$ with triethanolamine. *Dalton Transactions*, **43**, 941–944.

Grey, I.E., Mumme, W.G., MacRae, C.M., Caradoc-Davies, T., Price, J.R., Rumsey, M.S. and Mills, S.J. (2013) Chiral edge-shared octahedral chains in liskeardite, $[(Al,Fe)_{32}(AsO_4)_{18}(OH)_{42}(H_2O)_{22}]\cdot 52H_2O$, an open framework mineral with a pharmacoalumite-related structure. *Mineralogical Magazine*, **77**, 3125–3135.

Kampf, A.R., Hughes, J.M., Nash, B.P. and Marty, J. (2014*a*) New polyoxometalate minerals from the western United States. *21st General Meeting of the International Mineralogical Association, South Africa, 1–5 September, 2014*. Abstract Volume p. 374.

Kampf, A.R., Hughes, J.M., Nash, B.P. and Marty, J. (2014*b*) Kokinosite, $Na_2Ca_2(V_{10}O_{28})\cdot 24H_2O$, a new decavanadate mineral species from the St. Jude mine, Colorado: crystal structure and descriptive mineralogy. *The Canadian Mineralogist*, **52**, 15–25.

Kampf, A.R., Hughes, J.M., Nash, B.P., Wright, S.E., Rossman, G.R. and Marty, J. (2014*c*) Ophirite, $Ca_2Mg_4[Zn_2Mn^{3+}_2(H_2O)_2(Fe^{3+}W_9O_{34})_2]\cdot 46H_2O$, a new mineral with a heteropolytungstate tri-lacunary Keggin anion. *American Mineralogist*, **99**, 1045–1051.

Laugier, J. and Bochu, B. (2000) *LMGP-Program for the interpretation of X-ray experiments*. INPG/Laboratoire des Matériaux et du Génie Physique. St Martin d'Heres, France.

Long, De-L., Tsunashima, R and Cronin, L. (2010) Polyoxometalates: building blocks for functional nanoscale systems. *Angewandte Chemie, International Edition*, **49**, 1736–1758.

Mandarino, J.A. (1981) The Gladstone-Dale relationship: Part IV. The compatibility concept and its application. *The Canadian Mineralogist*, **19**, 441–450.

Lopez, X., Carbo, J.J., Bo, C. and Poblet, J.M. (2012) Structure, properties and reactivity of polyoxometalates: a theoretical perspective. *Chemical Society Reviews*, **41**, 7537–7571.

Sheldrick, G.M. (2008) A short history of SHELX. *Acta Crystallographica,* **A64**, 112–122.

Visser, J.W. (1969) A fully automated program for finding the unit cell from powder data. *Journal of Applied Crystallography,* **2**, 89.

Walenta, K. (1983) Bulachit, ein neues Aluminiumarsenatmineral von Neubulach im nordlichen Schwarzwald. *Aufschluss*, **34**, 445–451.